

# Application of Kubelka-Munk Theory in Device-independent Color Space Error Diffusion

*Shilin Guo and Guo Li*  
*Hewlett-Packard Company, San Diego Site*

## Abstract

Color accuracy becomes more critical for color inkjet printers, as their print quality improves to near photographic. However, due to pen to pen variance, the printed color of each individual printer may be different. This paper investigated a new printing process, which incorporated spectral models of inkjet ink mixing and the technology of vector error-diffusion in device-independent color space. No colormap building or colormapping process is necessary because color correction is built-in in the halftoning process. This process allows users to calibrate the printer and has the potential of faster processing of color images.

## Introduction

Until recently, most inkjet printers do not have the capability of self color calibration. Most printer drivers only allow users the ability to control curve shapes of RGB channels with sliders, based on the users' own impression of the prints. Such color calibration process was formalized in the HP PhotoSmart photo printer. A PhotoSmart printer user can interactively calibrate by printing numbers of gray images with various hue casts and contrast. The printer will automatically adjust color curves based on the best print picked by the user. In either of the above situations, print results depend heavily on users' preference and experience. For users lacking of experience in imaging or photography, color calibration is a painful job. In order to reproduce accurate color prints, it is necessary to have a self color calibration process independent of user's preference.

To compensate the color imbalance caused by the drop volume difference of inkjet pens, some detection has to be done either on the pen production line or at each individual printer. Calibrating pens on the production line does not reflect a pen's variance over its lifetime. Putting a sensor in each printer is an ideal way of approaching self color calibration. In this case, it is very important to extract the maximum amount of information from a simple device in order to minimize cost. Spectral modeling of mixing ink is a good technique in achieving this goal with fairly good accuracy.<sup>1</sup> It can be used to calculate the spectral data, and then the color, of any ink combination based on the information of several primary color tiles. Each primary color tile is prepared by printing each of the primary inks on paper, one drop per pixel.

Color images with continuous tone can be printed by rendering among available ink combinations. This process, as we know, is called halftoning process. In conventional color printers, color halftoning is usually conducted independently in C, M, Y and K components, which are printer-dependent color space. Input images need to be colormapped before the halftoning process. Colormapping controls the printed color by transferring device-independent color (such as CIELAB) or CRT-dependent color to printer-dependent color (printer RGB or CMYK).

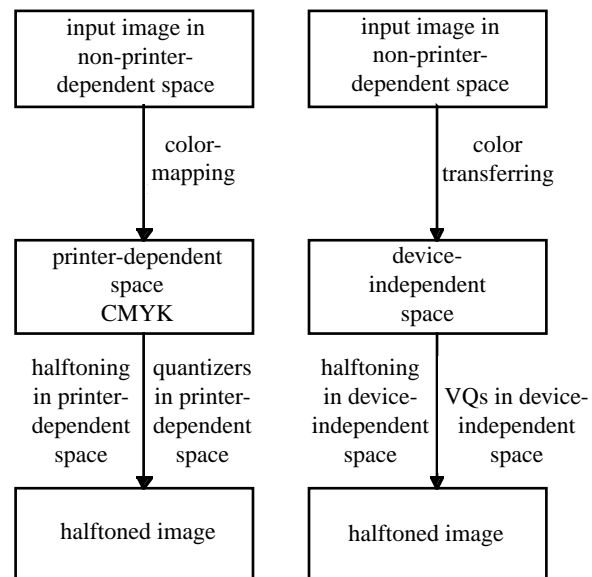


Figure 1. Color image processing pipeline with halftoning conducted in printer-dependent space (left) vs. in device-independent space (right)

Research<sup>5,7</sup> has been accomplished to explore the idea of halftoning in device-independent space, such as CIELAB and XYZ. These two approaches are shown in Figure 1. Vector error-diffusion (VED) is the most popular halftoning algorithm adopted in the second approach, where color of each available ink combinations can be imagined as vector quantizers (VQs) in a 3d space. In the case of traditional four-ink binary printers, there are only eight color VQs (white, cyan, magenta, yellow, red, green, blue, and black). The current multi-pass, multi-ink printing system allows thousands of ink combina-

tions to be printed without halftoning, or, it has thousands of VQs. These color vectors can be calculated with the spectral model described in the last paragraph.

As shown in Figure 1, colormapping will not be necessary if halftoning is conducted in device-independent space. This may save a significant amount of time in the color image processing pipeline, as color transferring is less time-consuming than 3d colormapping.

The proposed printing process will be described in the next part of this paper. After that, this paper reviews the spectral modeling of mixing ink, the technology of vector error diffusion, and their application in the proposed printing process. The last few sections of this paper will present experiments, followed by results and discussion.

## Proposed Method

In the proposed process, each printer has a light source, a sensor and three color filters. The reflectance spectra data  $R_{\text{prim\_normOnPaper}}$  of the standard primary tiles printed by nominal pens on a certain paper are measured by a spectrophotometer saved, as well as the reflectance spectra data  $R_{\text{paper}}$  of the same type of paper. The tiles' reflectance readings by the same type of light source, sensor, and proper filters are also saved as  $u$ . The following process is:

- Print primary test tiles with the test pens.
- The test tiles are then measured by the build-in sensor through proper color filters. Each color filter should be designed to be a narrow band-passing filter at the peak/valley wavelength of each primary ink's spectrum (excluding black ink).
- The scaling factor  $p$  is the ratio between the sensor's reading  $w$  on a primary test tile over sensor's reading  $u$  on the corresponding standard primary tiles.  $p$  is also called relative sensor reading. If the test pen has the same drop volume as nominal pen,  $p$  equals 1.0. In this subtractive printing system, if the test pen is a low drop volume pen,  $p$  is greater than 1.0. If the test pen is high drop volume pen and  $p$  is smaller than 1.0.
- By applying spectral modeling theory, the spectrum data and color can be calculated for all ink combinations.
- Using the color of ink combinations as VQs, conduct VED in device-independent color space.

## Spectral Modeling: Kubelka-Munk Theory

There are two types of spectral modeling theories: Bouguer-Beer Law for transparent substrate, and Kubelka-Munk (K-M) law for translucent and opaque substrate. For ink-jet printers, most color images were printed on opaque substrates, *i.e.*, plain paper, coated paper, or glossy photo paper. Therefore, we will only concentrate on Kubelka-Munk theory.

K-M theory models translucent and opaque substrates with two light channels traveling in opposite directions. The light is scattered and absorbed in only two directions, up and down. A background is presented at the bottom of the medium to provide the upward light

reflection, as shown in Figure 2. This theory was discussed in detail by Allen<sup>3</sup> for painting and textile industries. Later Kang<sup>1</sup> and Berns<sup>4</sup> applied K-M theory in inkjet printer and thermal transfer printer.

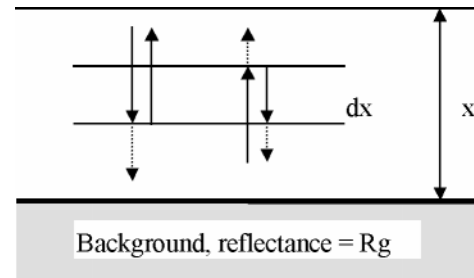


Figure 2. The K-M two channel model of the light absorption and scattering. (Adapted from reference 2)

The basic theory and derivations of K-M formula can be found in many publications<sup>2</sup>. Equations (1) through (4) were used by Henry Kang in reference 1. Equation (1) express two-constant K-M theory, in which parameters K and M are determined separately. R, S, and K are functions of wavelength. This equation can be simplified to single-constant theory (equation (2)) for opaque substrate. Reflectance spectra,  $R_{\text{inf}}$ , can be measured by spectrophotometer. Equation (3) is the re-arranged version of equation (2), and this equation is used to calculate the constant parameter,  $(K/S)_{\text{prim}}$  for each primary colors. Constant  $(K/S)_{\text{mix}}$  is predicted by equation (4), and the reflectance spectrum of a mixed color is obtained by equation (2).

$$R = \frac{1 - R_g [a - b \coth(bSx)]}{a - R_g + b \coth(bSx)} \quad (1)$$

R: reflectance of the film  
 $R_g$ : reflectance of background  
 K: the absorption coefficient  
 S: the scattering coefficient  
 $a = 1 + K/S$   
 $b = (a^2 - 1)^{1/2} = [(K/S)^2 + 2(K/S)]^{1/2}$   
 x: the film thickness

$$\coth(bSd) = \frac{\exp(bSx) + \exp(-bSx)}{\exp(bSx) - \exp(-bSx)}$$

$$R_{\text{inf}} = 1 + (K/S) - [(K/S)^2 + 2(K/S)]^{1/2} \quad (2)$$

$R_{\text{inf}}$ : reflectance at infinite thickness

$$(K/S)_{\text{prim}} = (1 - R_{\text{prim}})^2 / 2R_{\text{prim}} \quad (3)$$

$R_{\text{prim}}$ : Reflectance spectrum of paper or a primary color

$$(K/S)_{\text{mix}} = (K/S)_{\text{substrate}} + c_1(K/S)_{\text{prim}_1} + c_2(K/S)_{\text{prim}_2} + \dots + c_n(K/S)_{\text{prim}_n} \quad (4)$$

$c_1, c_2, \dots, c_n$ : concentration of the 1<sup>st</sup>, 2<sup>nd</sup>, and the  $n$ 'th primary color.

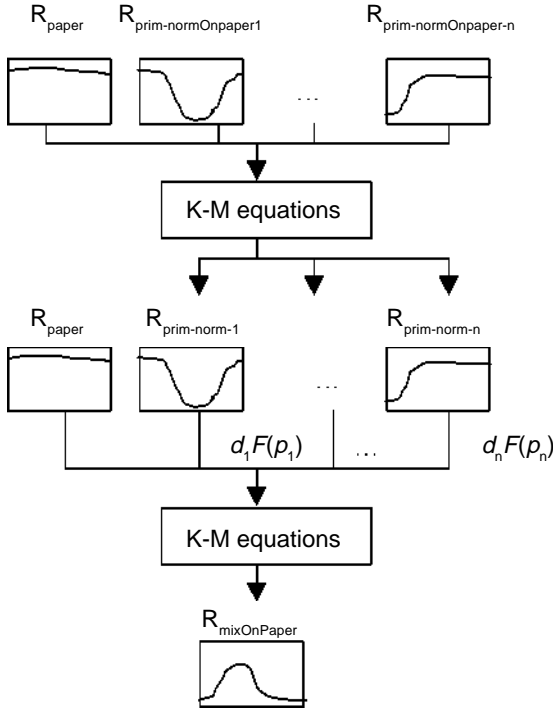


Figure 3. Apply K-M theory to predict spectrum of mixed inkjet ink from pre-measure spectrum of primary tiles

Figure 3 shows the process of applying K-M theory in ink-jet ink mixing. Outputs are spectra of the mixtures of primary inks on paper  $R_{\text{mixOnPaper}}$ . Inputs are:

- Reflective spectrum,  $R_{\text{paper}}$ , for the unimaged paper.  $R_{\text{paper}}$  is pre-measured and saved in the printing system.
- Reflective spectrum  $R_{\text{prim-normOnPaper}}$  for each primary ink tile.  $R_{\text{prim-normOnPaper}}$  is also pre-measured and saved.
- Relative sensor reading  $p$  for each primary tile.
- Drop number  $d$  of each primary ink in the mixed ink tile.

In this paper's application, equation (4) is modified to equation (5).

$$\begin{aligned} (K/S)_{\text{mixOnPaper}} = & (K/S)_{\text{paper}} + d_1 F(p_1) (K/S)_{\text{prim-norm-1}} + \\ & d_2 F(p_2) (K/S)_{\text{prim-norm-2}} + \dots + d_n F(p_n) (K/S)_{\text{prim-norm-n}} \quad (5) \\ c = & d \cdot F(p) \end{aligned}$$

$d_1, d_2, \dots, d_n$ : drop number per pixel of the 1<sup>st</sup>, 2<sup>nd</sup>, and the  $n$ 'th primary ink.

$p_1, p_2, \dots, p_n$ : relative sensor readings of the 1<sup>st</sup>, 2<sup>nd</sup>, and the  $n$ 'th primary tile.

Since both ink and paper contribute to  $R_{\text{prim-normOnPaper}}$ , we have to separate these two factors in the spectral modeling.  $(K/S)_{\text{prim-norm}}$  is calculated by equations (6) through (8). In equation (8), ink concentration  $c$  is set to one because primary tile has one-drop ink per pixel, and  $p$  equals to one. Once  $(K/S)_{\text{prim-norm}}$  is obtained,  $R_{\text{prim-norm}}$  can be calculated by equation (2).

$$(K/S)_{\text{paper}} = (1 - R_{\text{paper}})^2 / 2R_{\text{paper}} \quad (6)$$

$$(K/S)_{\text{prim-normOnPaper}} = (1 - R_{\text{prim-normOnPaper}})^2 / 2R_{\text{prim-normOnPaper}} \quad (7)$$

$$(K/S)_{\text{prim-norm}} = (K/S)_{\text{prim-normOnPaper}} - (K/S)_{\text{paper}} \quad (8)$$

For primary test tile, concentration  $c_{\text{prim-test}}$  is a function of  $p$ . As mentioned in previous section,  $p$  is defined as the ratio of  $R_{\text{prim-testOnPaper}}$  and  $R_{\text{prim-normOnPaper}}$  at a certain wavelength, and it is obtained from the proposed built-in sensor. Equations (9) through (12) derive the function  $F(p)$ .

$$(K/S)_{\text{prim-test}} = c_{\text{prim-test}} (K/S)_{\text{prim-norm}} \quad (9)$$

$$\begin{aligned} C_{\text{prim-test}} = F(p) = & \frac{(K/S)_{\text{prim-test}}}{(K/S)_{\text{prim-norm}}} \\ = & \frac{(K/S)_{\text{prim-testOnPaper}} - (K/S)_{\text{paper}}}{(K/S)_{\text{prim-normOnPaper}} - (K/S)_{\text{paper}}} \quad (10) \\ = & \frac{(1 - R_{\text{prim-testOnPaper}})^2 / 2R_{\text{prim-testOnPaper}} - (K/S)_{\text{paper}}}{(1 - R_{\text{prim-normOnPaper}})^2 / 2R_{\text{prim-normOnPaper}} - (K/S)_{\text{paper}}} \end{aligned}$$

$$R_{\text{prim-testOnPaper}} = pR_{\text{prim-normOnPaper}} \quad (11)$$

$$\begin{aligned} C_{\text{prim-test}} = F(p) \quad (12) \\ = & \frac{(1 - pR_{\text{prim-normOnPaper}})^2 / 2pR_{\text{prim-normOnPaper}} - (K/S)_{\text{paper}}}{(1 - R_{\text{prim-normOnPaper}})^2 / 2R_{\text{prim-normOnPaper}} - (K/S)_{\text{paper}}} \end{aligned}$$

So far, we have prepared everything for equation (5) to calculate  $(K/S)_{\text{mixOnPaper}}$ . The last step is a simple calculation of reflectance spectrum  $R_{\text{mixOnPaper}}$  by Equation (2).

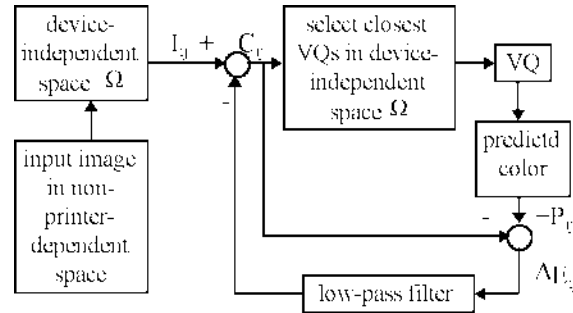


Figure 4. Vector Error-diffusion (VED) process

### Vector Error-Diffusion (VED) in Device-independent Space

VED is similar to the standard error-diffusion process, except it happens in 3-dimensional space. The process conducted in a general device-independent color space  $\Omega$  is shown in figure 4. First, the color  $I_{ij}$  of a selected pixel in input image is transferred into the space  $\Omega$  by assuming a certain CRT model. The color vector  $I_{ij}$  is then combined with the error vectors  $\Delta E_{ij}$  propagated

from previous pixels. The modified input color  $C_{ij}$  is compared to all the color VQs in the space  $\Omega$ . The color VQ closest to  $C_{ij}$  is chosen. This, in turn, means the corresponding ink combination and color  $P_{ij}$  is chosen for the selected pixel. In the next step, the error vector  $DE_{ij}$  between the modified input  $C_{ij}$  and  $P_{ij}$  will be propagated to neighboring pixels based on certain error-diffusion weights.

## Experiment

K-M spectral model was exercised on HP Photosmart Photo printer and HP Photosmart Glossy photo paper. HP PhotoSmart Photo printer is a 300dpi multi-pass printer with six primary ink channels: black (K), yellow (Y), dark cyan (Cd), light cyan (Cl), dark magenta (Md), and light magenta (Ml) inks. In this work, the printer's driver was by-passed so that we can prepare test samples that are exactly what we want.

Each primary color tile was prepared by printing each of the six primary inks on HP PhotoSmart Glossy Photo Paper, one drop per pixel. Full area coverage was obtained, since the single dot size was big enough to cover a 300 dpi pixel. The test target includes thousands of uniform color tiles, which are the mixture of primary inks with known number of drops ( $d_K, d_Y, d_{Cd}, d_{Cl}, d_{Md}, d_{Ml}$ , range from 0 to 4) of each primary ink per pixel.

The primary color tiles and paper's reflective spectra,  $R_{\text{prim-normOnPaper}}$  and  $R_{\text{paper}}$ , were measured by a Gretag Spectro-photometer SPM50, wavelength from 380nm to 730nm. Constant  $(K/S)_{\text{prim-norm}}$  was calculated by equation (8), and  $(K/S)_{\text{mixOnPaper}}$  was calculated by equation (5). Reflectance spectrum of multi drops of one primary ink or the mixture of primary inks,  $R_{\text{mixOnPaper}}$  were calculated by equation (2).

K-M model needs a correction for the refractive index that changes between air and a colored layer. This paper used constant correction, in which constant surface reflection is subtracted from the measured reflectance,  $R_{\text{inf}}$  (equation (13)).

$$R_{\text{inf}} = R_m - R_s \quad (13)$$

$R_m$ : measured reflective spectrum  
 $R_s$ : a constant representing the surface reflection

In Kang's approach, a single constant  $R_s$  was used to fit data for all wavelength. To get the best results, we divided spectrum into four segments in this paper. Each segment had its own constant  $R_s$ . Our approach can be explained by the fact that refractive index changes with wavelength.

$\Delta E$  in CIELAB and the spectra difference between measured and predicted colors for each ink combination were also calculated. The algorithm was implemented in a C program.

Calculated  $R_{\text{mixOnPaper}}$  of each ink combination was also transferred to selected device-independent spaces. About one thousand ink combinations all over the color space are chosen as VQs. The colors for all VQs are properly scaled to ensure using paper color as white point. VED has been conducted in CIELAB and sRGB color

space. sRGB is a newly proposed device-independent color space standard based on a well-defined virtual CRT.

Because of its character of perceptually uniformity, CIELAB color space is a good start for reducing dithering granularity. In this paper, in order to further reduce graininess, a modified CIELAB space is actually used, where  $L^*$ ,  $a^*$ , and  $b^*$  are weighted differently when calculating the Euclidean distance between modified color  $C_{ij}$  and color VQs. The optimal weight ratio depends on printer resolution, ink dot size and concentration. In contrast to CIELAB, XYZ color space is a linear space, which tends to better preserve the color accuracy during VED process. However, experiments<sup>7</sup> have shown that VED conducted in XYZ is just slightly better than in CIELAB in terms of color accuracy.

When VED is conducted in CIELAB, the RGB values of input image need to be transferred into CIELAB according to sRGB standard. No extra step for color matching is needed. When VED is conducted in sRGB space, not even color transferring is needed. Thus, the whole printing pipeline is further simplified.

## Results and Discussion

### Result of Predicting Color for Ink Combinations

Average  $\Delta E$  is 6.0 for all the uniform color tiles used in VED, excluding paper and 6 primaries. The predicted and measured color are metameric pairs because their color in  $L^*a^*b^*$  space were very close but spectra were not exactly the same. However, the average spectra difference was less than 1%. Figure 6 is an example experimental result. These numerical data results were comparable to previous works by Berns and Kang, but this work still made a big improvement because Berns and Kang only included 10 to 30 color tiles in their modeling work, which can not be applied in CIELAB space error diffusion.

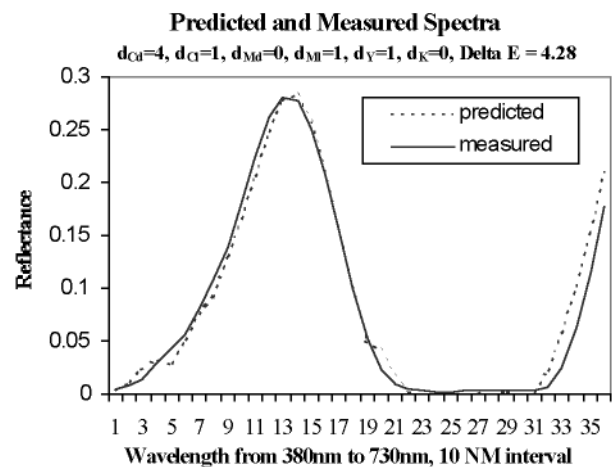


Figure 6. An example of metameric pair, predicted and measured spectra

### Result of Color Accuracy of the Whole Printing Pipeline

To evaluate the accuracy of color reproduction,  $9 \times 9 \times 9 = 729$  evenly spaced RGB color tiles are printed

through the VED process. The process conducted in CIELAB is indicated by figure 7. sRGB is assumed as the CRT standard when calculating the predicted CIELAB from input RGB. The predicted CIELABs are then compared to the measurement of the real print. An average  $\Delta E$  of 13.46 is achieved for all the 729 tiles. As a significant portion of desired color are out of printing gamut, the average  $\Delta E$  is 6.26 for tiles within gamut.

When the VED is conducted in sRGB space, an average DE of 17.67 is achieved for all the 729 tiles. The average DE is 8.83 for tiles within gamut. The prints are less grainy.

## Discussion

As we know, the shape of inkjet dots is not perfectly square. The size of inkjet dot also increases with increasing number of ink drops per pixel. A large number of ink drops on a specific pixel will tend to cover part of the area of neighboring pixels. This has no impact on uniform area where every pixel uses the same ink combination. However, when the neighboring pixel uses a different ink combination, the color of neighboring pixels will be changed. Various printing models have been developed to compensate for these specific characteristics of binary printers. These models may be used in the VED step of assigning a color to a selected pixel from the chosen VQ. However, the situation becomes even more complicated for multi-channel, multi-pass inkjet system because of the large amount of ink combinations.

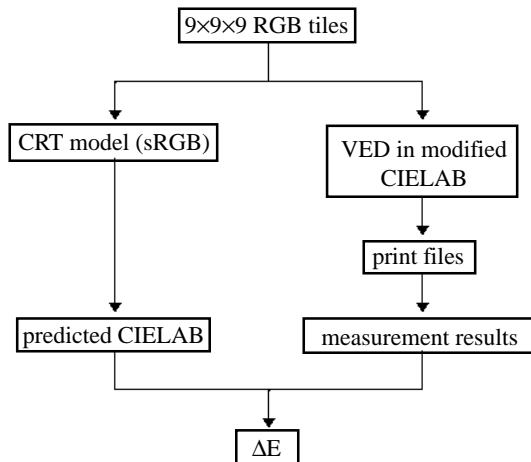


Figure 7. Evaluate the color accuracy of the whole printing process

Although, some error exists in the printing pipeline, they are systematic and stable. Once the K-M model is well established, color balance of the output depends solely on the sensor reading. It means that an individual user can perform color calibration efficiently.

## Acknowledgements

The authors would like to acknowledge their debt to all colleagues who helped make this study possible. Thanks to Frank Bockman and Mark Wisnosky for the managerial support and for their helpful suggestions. We also want to express our gratitude to John F. Meyer for reviewing the draft.

## References

1. Henry Kang, Kubelka-Munk modeling of ink jet ink mixing, *Journal of Imaging Technology*, Vol. 17, Num. 2, April/May 1991.
2. Kubelca, New Contribution to the optics of intensely light-scattering materials:Part I, *Journal of Opt. Soc. Am.*, 38:448-457, 1948.
3. Eugene Allen, Color formulation and shading, in *Optical Radiation Measurements*, Vol. 2, Chap. 7, F. Grum and C. J. Bartleson, Eds., Academic Press, New York, NY, 1980, pp. 296-315.
4. Roy Berns, Spectral modeling of a dye diffusion thermal transfer paper, *Journal of Electronic Imaging*, Oct., 1993, Vol. 2(4).
5. Kim, S. Kim, Y. Seo, I. Kweono, Model Based Color Halftoning Techniques On Perceptually Uniform Color Spaces, *Proceeding of IS&T's 47th Annual Conference*, 1994, Rochester, New York; see *Recent Progress in Digital Halftoning, Vol. 1, pg. 68*.
6. B. W. Kolpatzik, C. Bouman, Color Paletter Design for Error Diffusion, *Proceedings of IS&T's 46th Annual Conference*, 1993, Cambridge, Massachusetts; see *Recent Progress in Digital Halftoning, Vol. 1, pg. 103*.
7. Haneishi, N. Shibukatsu, Y. Miyake, Color Digital Halftoning for Colorimetric Color Reproduction, *Proceedings of IS&T's Tenth International Congress on Advances in Non-Impact Printing Technologies*, 1994, New Orleans, Louisiana; see *Recent Progress in Digital Halftoning, Vol. 1, pg. 9*.

\* Previously published in *IS&T's 1998 PICS Conference Proc.*, pp. 344-348, 1997.